This article is published as part of the *Dalton Transactions* themed issue entitled:

Contributions of Inorganic Chemistry to Energy Research

Guest Editors Duncan Wass and Neil Robertson
University of Bristol and University of Edinburgh, UK

Published in issue 15, 2011 of *Dalton Transactions*

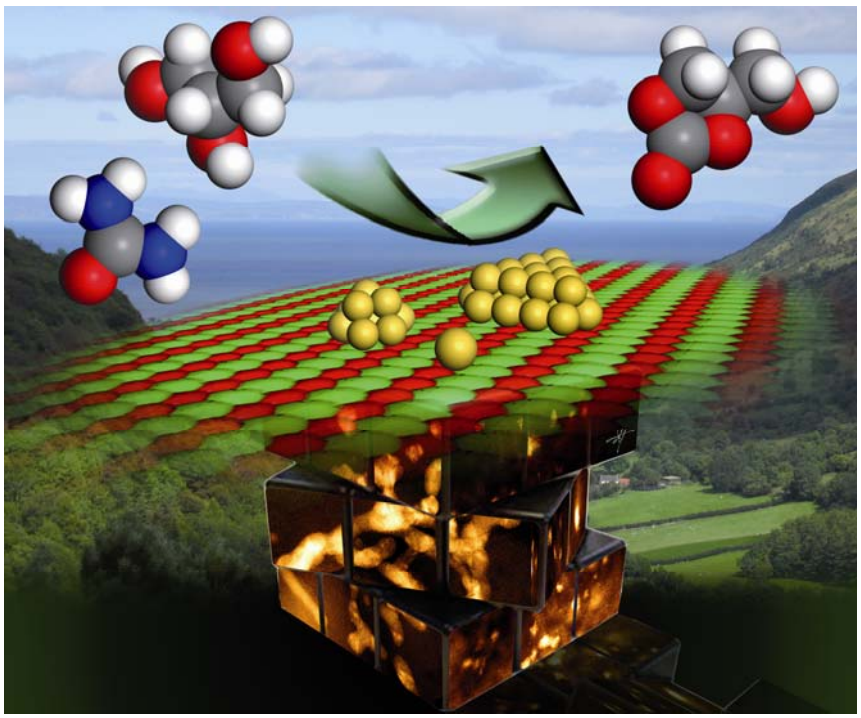

Image reproduced with permission of Graham Hutchings

Articles in the issue include:

ARTICLES:

Dalton Transactions

An international journal of inorganic chemistry

www.rsc.org/dalton

Volume 40 | Number 15 | 21 April 2011 | Pages 3761–3996

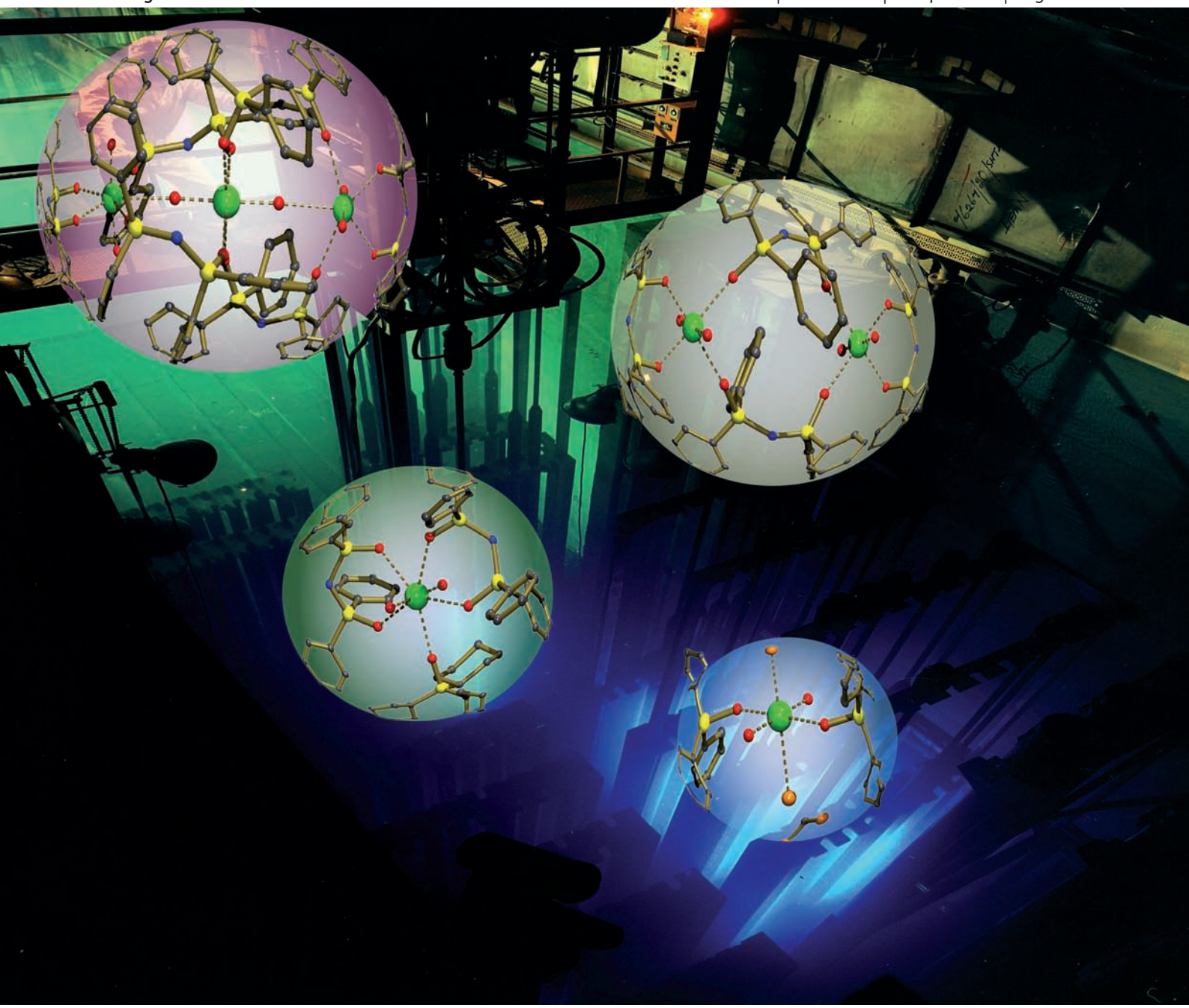

ISSN 1477-9226

RSC Publishing

COVER ARTICLE

Cornet and Natrajan *et al.*

Probing the local coordination environment and nuclearity of uranyl(VI) complexes in non-aqueous media by emission spectroscopy

Dalton Transactions

Cite this: *Dalton Trans.*, 2011, **40**, 3914

www.rsc.org/dalton

PAPER

Probing the local coordination environment and nuclearity of uranyl(VI) complexes in non-aqueous media by emission spectroscopy†

Michael P. Redmond, Stephanie M. Cornet,* Sean D. Woodall, Daniel Whittaker, David Collison, Madeleine Helliwell and Louise S. Natrajan*

Received 25th October 2010, Accepted 30th November 2010
DOI: 10.1039/c0dt01464h

We describe the synthesis, solid state and solution properties of two families of uranyl(VI) complexes that are ligated by neutral monodentate and anionic bidentate P═O, P═NH and As═O ligands bearing pendent phenyl chromophores. The uranyl(VI) ions in these complexes possess long-lived photoluminescent LMCT $^3\Pi_u$ excited states, which can be exploited as a sensitive probe of electronic structure, bonding and aggregation behaviour in non-aqueous media. For a family of well defined complexes of given symmetry in *trans*-$[UO_2Cl_2(L_2)]$ (L = Ph_3PO (**1**), Ph_3AsO (**2**) and Ph_3PNH (**3**)), the emission spectral profiles in CH_2Cl_2 are indicative of the strength of the donor atoms bound in the equatorial plane and the uranyl bond strength; the uranyl LMCT emission maxima are shifted to lower energy as the donor strength of L increases. The luminescence lifetimes in fluid solution mirror these observations (0.87–3.46 μs) and are particularly sensitive to vibrational and bimolecular deactivation. In a family of structurally well defined complexes of the related anion, tetraphenylimidodiphosphinate (TPIP), monometallic complexes, $[UO_2(TPIP)(thf)]$ (**4**), $[UO_2(TPIP)(Cy_3PO)]$ **5**), a bimetallic complex $[UO_2(TPIP)_2]_2$ (**6**) and a previously known trimetallic complex, $[UO_2(TPIP)_2]_3$ (**7**) can be isolated by variation of the synthetic procedure. Complex **7** differs from **6** as the central uranyl ion in **7** is orthogonally connected to the two peripheral ones *via* uranyl → uranium dative bonds. Each of these oligomers exhibits a characteristic optical fingerprint, where the emission maxima, the spectral shape and temporal decay profiles are unique for each structural form. Notably, excited state intermetallic quenching in the trimetallic complex **7** considerably reduces the luminescence lifetime with respect to the monometallic counterpart **5** (from 2.00 μs to 1.04 μs). This study demonstrates that time resolved and multi-parametric luminescence can be of value in ascertaining solution and structural forms of discrete uranyl(VI) complexes in non-aqueous solution.

Introduction

The chemistry of uranium is currently enjoying a renaissance, in part, due to recent reports detailing synthetic routes to useful starting materials which provide convenient entry points into uranium coordination chemistry,[1] and more recently in response to the increasing impact of nuclear power in a societal balanced energy portfolio;[2] this includes new builds, decomissioning schemes and waste management agendas. The chemistry of uranium itself, is unique, with the fully oxidised +6 oxidation state $\{UO_2\}^{2+}$ being the most prevalent and well studied species. One of the most intriguing properties of $\{UO_2\}^{2+}$, which sets it apart from the +III, +IV and +V valence states, is its distinctive optical properties.

The optical properties of uranyl(VI) compounds have been known for over 150 years;[3] they were first investigated in yellow–green uranium containing glasses and minerals[4,5] and subsequently in synthetic analogues often in aqueous conditions.[6] The absorption and emission profiles of uranyl(VI) salts are highly characteristic;[7] they possess a high density of 12 excited states,[8] frequently observed in the absorption spectra, and display bright green luminescence centered around 520 nm.[9] This emission often exhibits considerable fine structure in the solid state and in aqueous solution as a result of strong coupling of the ground state symmetric vibrational O═U═O (ν_1) mode with the $^3\Pi_u$ electronically excited state.[10] For example, in simple salts such as uranyl perchlorate, sulfate, carbonate and nitrate, up to six of these 'hot bands' are commonly observed.[11] The emission profile itself is ligand-to-metal charge transfer (LMCT) in origin, arising from promotion of an electron from an 'yl' bonding orbital (σ_u,

School of Chemistry, The University of Manchester, Oxford Road, Manchester, UK, M13 9PL. E-mail: louise.natrajan@manchester.ac.uk; Fax: +44 (0)161 275 4616; Tel: +44 (0)161 275

† Electronic supplementary information (ESI) available: crystallographic information and thermal ellipsoid plot of **7**, Raman spectra of the complexes, V-T NMR spectra of **4** and **5** and absorption, emission and excitation spectra of the complexes. CCDC reference numbers 798349–798352. For ESI and crystallographic data in CIF or other electronic format see DOI: 10.1039/c0dt01464h

σ_g, π_u and π_g) to a non-bonding uranium $5f_\delta$ and $5f_\phi$ orbital.[12] Accordingly, this CT transition is formally a Laporte forbidden process, where relaxation of the selection rule is dependent upon the local symmetry and coordination environment around the uranium cation and the spin orbit coupling parameter. As a result, the electronic excited state of $\{UO_2\}^{2+}$ is rather long lived, with radiative lifetimes in the solid state and frozen solution typically of the order of hundreds of microseconds. In addition, a ligand-to-metal charge transfer transition arising from promotion of an electron of an equatorial bound donor atom to the uranium centre is often observed.

Experimental[13] and density functional theory calculations,[14] have demonstrated that the excited uranyl(VI) ion can readily undergo photoreduction in aqueous and methanolic media. Quenching of the LMCT emission arises from an electron transfer process involving a uranyl(V) radical pair. In these cases, the excited triplet state is stabilised by hydrogen bonding interactions, often resulting in H atom abstraction and a significant participation of non-radiative decay in the fate of the excited state. In the absence of suitable substrates, the highly oxidising and reducing $\{UO_2^{2+}\}^*$ excited state undergoes a radical pair recombination, regenerating the singlet ground state and giving rise to typical uranyl(VI) emission profiles. Quenching processes in such scenarios are either bimolecular and/or vibronic in nature. In this case, the luminescence of uranyl(VI) can be exploited in ratiometric type assays and probes,[15] in an analogous fashion to which the visible emission of lanthanide(III) ions has been utilised.[16]

Whilst the luminescence of uranyl salts in aqueous media has been explored in detail, similar studies of uranyl complexes bearing organic-based ligands in protic solvents remain relatively uncommon.[17] The principal reason for this, is that the majority of organic complexes are not emissive at room temperature in fluid solution.[18,19] The π–π* and *n*–π* absorption transitions of common organic ligands (historically, β-diketonates and Schiff bases) overlap significantly with the uranyl emission spectrum; the uranyl emission is quenched by thermally-activated back energy transfer to low-lying excited states of the ligand. This can be rationalised since a marked temperature dependent behaviour on the emission is observed.

Interestingly, there are very few reports of uranyl photophysical investigations in non-aqueous solutions. This is perhaps surprising given the importance of uranium in separation processes such as the PUREX process (*P*lutonium and *U*ranium *R*efinement by *Ex*traction),[20] and considering its potential utility as a spectroscopic tool in uranium coordination chemistry. Moreover, multimetallic actinyl containing species are important in liquid–liquid extraction processes in non-aqueous media, yet their precise role remains undetermined.[21] We therefore reasoned that by correct choice of chromophore containing ligand, whereby the absorption envelope is restricted to the UV, the energy gap between the organic triplet excited state and the uranyl excited state would be large enough (≥ 1850 cm^{-1}) to obviate thermally activated back energy transfer and non-radiative decay processes.[22] In other words, spectral non-overlap of the emission and absorption spectra of the ligand and uranyl ion respectively. This, in turn, would give rise to strongly emissive compounds in aerated solution at room temperature. In this way, the observed spectral forms would lead to a useful probe of the local coordination environment of uranyl(VI) complexes, including geometry, the nature of the uranyl and ligand to metal bonding in the equatorial plane and the complex nuclearity.[41,42]

Results and discussion

We report here, for the first time, how a series of structurally related uranyl(VI) monomeric complexes containing phosphine oxide, arsine oxide and phosphinimine donor moieties can be differentiated from one another by time-resolved emission spectroscopy in non-aqueous solution under ambient conditions. We also demonstrate how, for a given ligand with the correct electronic properties, a trimetallic species can be distinguished from its monometallic and bimetallic counterparts.

Synthesis of uranyl(VI) complexes with monodentate ligands, $[UO_2Cl_2(L)_2]$ (1–3)

The first series of ligands we chose for this study form neutral organic soluble adducts with uranyl(VI) of the formula $[UO_2Cl_2(L)_2]$ (Scheme 1). Variation of the ancillary ligand, L in these complexes enables a systematic correlation of ligand electronic effects with emissive properties for a given symmetry (approximately D_{2h}) and where the complex speciation is known. Importantly, the ligands chosen for complexation with uranyl(VI) are able to afford complexes amenable to photophysical studies since they possess peripheral phenyl chromophores whose absorption envelope does not extend much beyond 260 nm (Schemes 1 and 2). These ligands can also be considered simple mimics for complexants in uranium extraction processes.

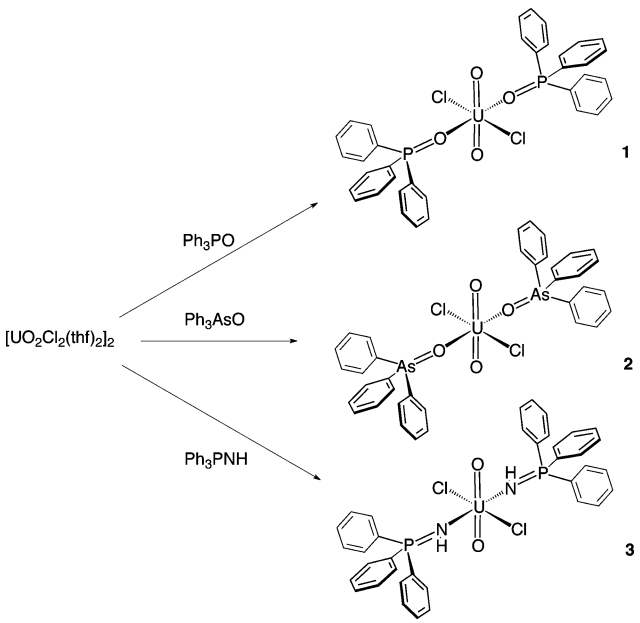

Scheme 1 Synthetic route to complexes **1**, **2** and **3**.

Under inert atmospheric conditions, displacement reactions of the neutral monodentate ligands triphenylphosphineoxide ($Ph_3P{=}O$), triphenylarsineoxide ($Ph_3As{=}O$) and triphenylphosphinimine ($Ph_3P{=}NH$)[23] with the labile thf molecules in uranyl chloride, $[UO_2Cl_2(thf)_2]_2$,[24] gave after workup and recrystallisation from CH_2Cl_2, yellow crystalline samples of *trans*-$[UO_2Cl_2(Ph_3PO)_2]$[25] (**1**), *trans*-$[UO_2Cl_2(Ph_3AsO)_2]$ (**2**) and

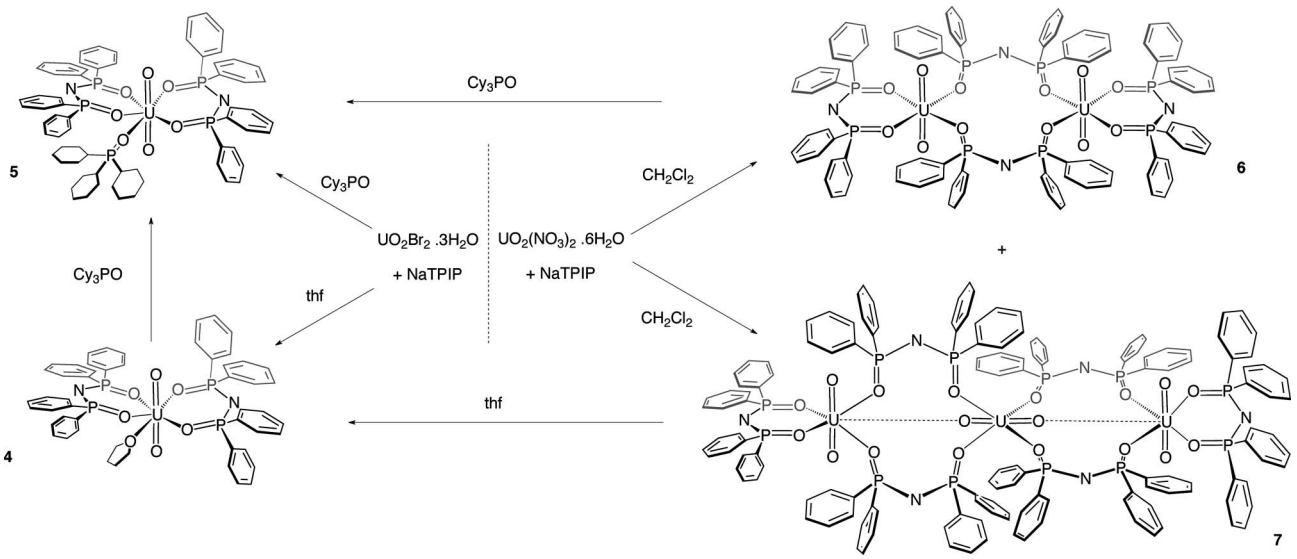

Scheme 2 Synthetic routes to complexes **4–7**.

trans-$[UO_2Cl_2(Ph_3PNH)_2]$ (**3**)[23] in adequate yield, (Scheme 1). The phosphinimine N-donor Ph_3PNH itself and its tris-cyclohexyl counterpart have been utilised to study disparities in covalency in metal–ligand bonding in the system $[UO_2Cl_2((H)XPR_3)_2]$ (X = O, N; R = Cy, Ph). The rationale for the particularly short U–N bond distances found in the complexes *trans*-$[UO_2Cl_2(HNPR_3)_2]$ (R = Cy, 2.392(5) Å;[26] Ph, 2.370(1) Å[23]) was found computationally to be a result of an increased amount of covalent character in the U–N bond in comparison to the phosphine oxide counterpart (**1**). We therefore reasoned that a spectroscopic study of these complexes would provide a complementary insight into the nature of the metal–ligand bonding interactions in uranyl(VI) complexes.

In solution, a mixture of the thermodynamic (*cis*-ligand) and kinetic isomers (*trans*-ligand) of **1**, **2** and **3** are observed by ^{31}P NMR spectroscopy, with the *trans*-isomer being dominant.[27] These isomers are not inconvertible on the timescale of the NMR experiment at room temperature since two sets of resonances are observed corresponding to each isomer.

X-ray crystal structure of *trans*-$[UO_2Cl_2(Ph_3AsO)_2]\cdot 2CH_2Cl_2$ (2)

The X-ray crystal structures of the complexes *trans*-$[UO_2Cl_2(Ph_3PO)_2]$[25] (**1**) and *trans*-$[UO_2Cl_2(Ph_3PNH)_2]$[23] (**3**) have previously been reported, the latter by us (CCDC reference codes CDXUPO01 and HAXZUC, respectively). We now report the single crystal X-ray crystal structure of the chloride derivative of $[UO_2Cl_2(Ph_3AsO)_2]$ (**2**), Fig. 1.

In **2**, the uranium cation is six coordinated, with the chloride and triphenylarsine oxide ligands lying in mutually *trans* positions about the uranium centre, which itself lies on a crystallographic inversion centre. The chloride and triphenylarsine oxide ligands occupy the equatorial plane of the distorted octahedron in a planar fashion and the uranyl oxo groups complete the coordination octahedron and lie in the axial positions. The equatorial ligands lie precisely in a plane, due to the centre of symmetry at the U atom. The interatomic distances (Table 2) compare well to those reported for *trans*-$[UO_2Cl_2(Ph_3PO)_2]$ and *trans*-$[UO_2Br_2(Ph_3AsO)_2]$,[27] *d*(U–Cl) = 2.671(4) Å and *d*(U-OAsPh$_3$) = 2.247(9) Å. The uranyl

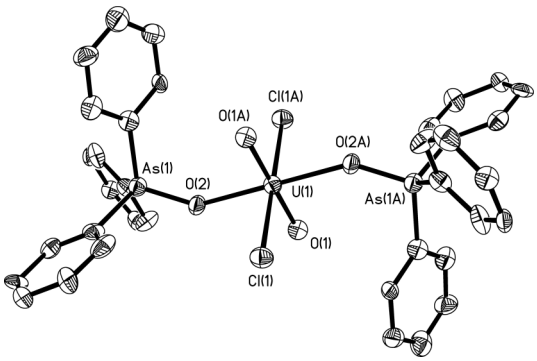

Fig. 1 Thermal ellipsoid drawing of $[UO_2Cl_2(Ph_3AsO)_2]$ (**2**) at the 50% probability level. H atoms omitted for clarity.

oxygen–metal bond distances are statistically indistinguishable at 1.760(9) Å and lie in the range of distances reported for similar uranyl(VI) halide complexes. The uranyl group itself is perfectly linear with a O–U–O angle measured as 180.0°.

Photophysical properties of complexes 1–3

The electronic absorption spectra of the complexes **1–3** in CH_2Cl_2 solutions display three main features; an intense band centered at 240 nm (*cf.* Fig. S5†), assigned to a spin allowed ligand centered π–π* transition within the phenyl chromophores; a broad feature at *ca.* 300 nm, arising from a ligand-to-metal charge transfer (LMCT) transition from an equatorial bound donor atom to the uranium cation and a weak transition at *ca.* 420 nm assigned to the Laporte forbidden $O_{yl} \rightarrow U$ LMCT transition ($\varepsilon \approx 50$ M cm^{-1}). The latter exhibits the well resolved vibrational fine structure typical of uranyl(VI) compounds.†

Excitation into either of these three absorption bands (260–460 nm), produces luminescence spectra which are dominated by the corresponding LMCT emission bands at *ca.* 400 nm and *ca.* 520 nm respectively. Interestingly, no emission resulting from fluorescence of the aromatic chromophores is observed in any of the systems studied. For comparison, the luminescence

Table 1 Photophysical properties of the complexes in CH_2Cl_2 in air-equilibrated solution at 295 K following 405 nm excitation

Complex	λ_{abs} (nm)[b]	λ_{em} (nm)[b,d]	$E_{0\text{-}0}$(cm^{-1})[e]	τ_1 (ns)[d,f]	τ_2 (ns)[d,f]	k_1 (10^6 s^{-1})	χ^2	ϕ ($\times 10^{-2}$))[h]
$[UO_2Cl_2(thf)_2]_2$[a]	[c]	504	[c]	150 (46%)	40 (54%)	6.67	1.52	[c]
1	428	529	19 860	1040 (75%)	130 (25%)	9.62	1.00	[c]
2	425	531	19 720	3460 (100%)	[g]	0.29	1.10	[c]
3	[c]	517	20 060	870 (93%)	190 (7%)	1.15	1.06	[c]
4	429	523	20 040	600 (100%)	[g]	0.17	1.09	0.05
5	425	521	19 920	2000 (100%)	[g]	0.50	1.01	0.28
6	429	531	19 670	1080 (100%)	[g]	0.92	1.01	0.09
7	431	532	19 650	1040 (100%)	[g]	0.96	1.04	0.13

[a] Values measure in thf solution. [b] Uranyl O→U LMCT. [c] Value not measured in this work, or could not be determined. [d] Identical results within error were determined at 375 nm excitation. [e] Apparent $E_{0\text{-}0}$ measured from emission spectra in cm^{-1}. [f] Lifetimes quoted at 405 nm excitation using a 450–550 nm bandpass interference filter and are subject to ± 10% error. [g] No secondary exponential component required to fit the kinetic trace. [h] Quantum yields determined relative to quinine sulfate in 1 M H_2SO_4 at 350 nm excitation, $\phi = 0.58$ at 295 K; estimated error ± 20%

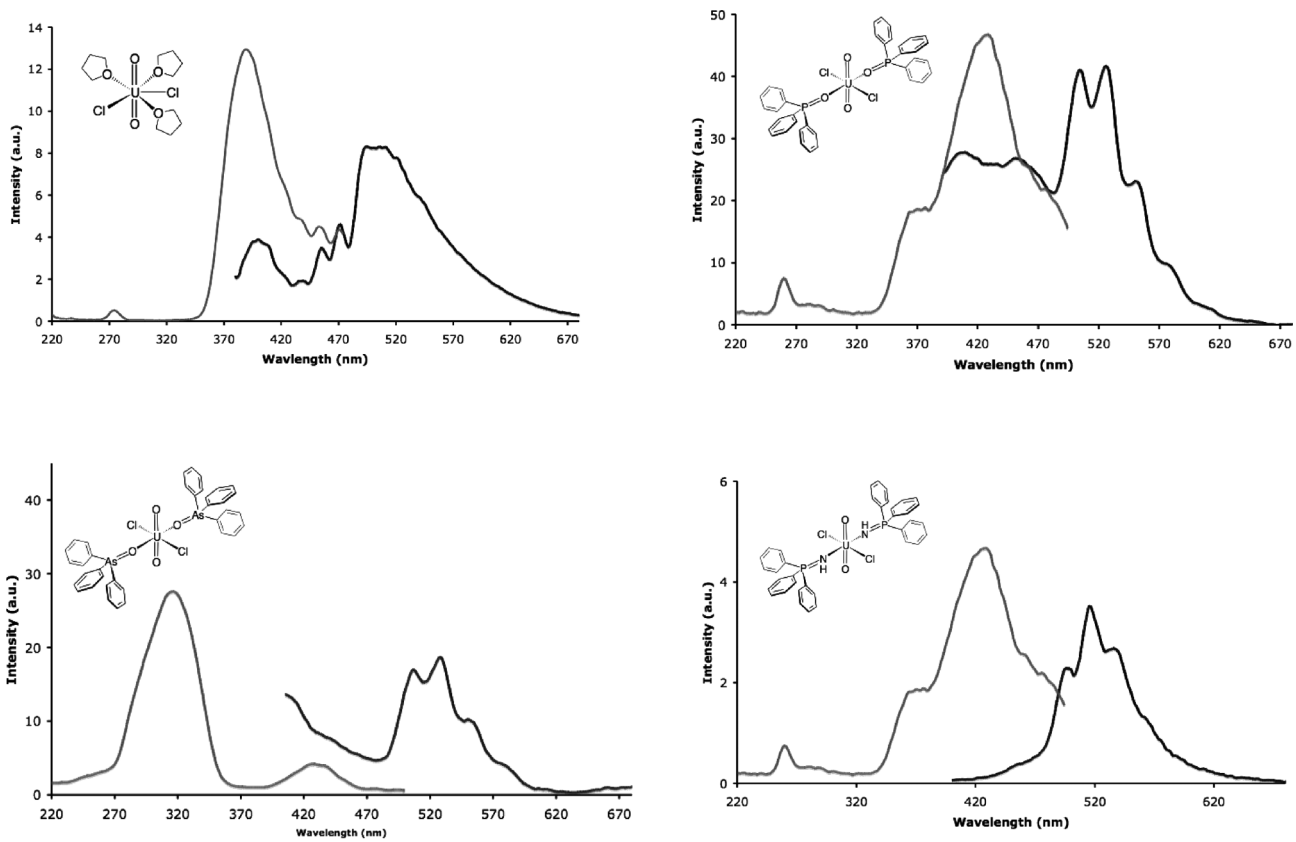

Fig. 2 Steady state emission following excitation at 360 nm (295 K), (black traces) and excitation spectra (grey traces) of $[UO_2Cl_2(thf)_2]_2$ in thf and the complexes **1–3** in air-equilibrated CH_2Cl_2. The emission centered at *ca.* at 420 nm is assigned as the equatorial donor to uranium LMCT and the emission centered at *ca.* 520 nm is the uranyl U═O LMCT emission. The spectral profiles are similar following 375, 405 and 420 nm excitation.

spectrum of the parent compound $[UO_2Cl_2(thf)_2]_2$ was recorded (Table 1). The emission in all complexes is essentially independent of excitation wavelength and the visible uranyl LMCT band is observed in the spectra irrespective of whether the phenyl group, the equatorial ligand to uranium LMCT or the uranyl LMCT itself is irradiated. However, the relative contributions of the L→U LMCT (L = Cl, Ph_3PO, Ph_3AsO, Ph_3PNH) and the uranyl $O_{yl'}$→U LMCT bands vary depending on the nature of the bound donor group. The excitation spectra of all complexes (recorded at the respective emission maxima) additionally confirm that the phenyl groups play a negligible role in the resultant emission profiles. The emission spectra exhibit features attributable to both LMCT transitions but show no π–π^* absorption transitions (Fig. 2). In contrast to organic complexes of the lanthanides, the emission is not sensitised by pendent aromatic groups, but instead, sensitised by the equatorial L→U LMCT or is a result of direct excitation of the uranyl unit itself (depending on the excitation wavelength used).

The emission maxima of the uranyl LMCT bands themselves are more informative than the corresponding absorption spectra and crudely are shifted to lower energy as the donor strength of the ancillary ligand increases. They follow the order [*trans*-$[UO_2Cl_2(Ph_3PNH)_2]$, < *trans*-$[UO_2Cl_2(Ph_3PO)_2]$, < *trans*-$[UO_2Cl_2(Ph_3AsO)_2]$ (517 nm, 529 nm, 531 nm respectively). This

Table 2 Selected interatomic distances (Å) and angles (°) for the complexes **2**, **4**, **5** and **6**

[a]	**2**·2CH_2Cl_2	**4**.thf	**5**·0.5Et_2O	**6**·3CH_2Cl_2
U═O	1.775(10)	1.774(2), 1.779(2)	1.769(3), 1.773(3)	1.799(11), 1.800(11)
U–O(L1)	2.248(9)	2.323(2), 2.373(2)	2.394(3), 2.367(3)	2.294(11)
U–O(L2)	2.248(9)	2.315(3), 2.402(2)	2.395(3), 2.415(3)	2.256(11)
U–X	2.671(4)	2.504(2)	2.329(3)	—
U–O(L3)	—	—	—	2.267(11), 2.237(12)
O═U═O	180.0(6)	175.97(11)	179.90(17)	178.9(7), 179.3(7)
O═U–O(L1)	89.1(4), 90.9(4)	89.88(10), 87.54(11), 87.54(11), 91.33(11)	91.31(13), 88.74(13), 87.89(13), 92.04(13)	87.7(5), 91.4(5)
O═U–O(L2)		88.51(10), 94.63(10), 95.38(11), 85.44(11)	91.42(13), 88.48(13), 90.57(13), 89.44(13)	90.5(5), 90.1(5)
O═U–O(L3)	—	—	—	91.1(5), 89.6(5), 89.1(5), 90.4(5)
O═U–X	89.9(3), 89.0(3), 91.0(3)	82.55(10), 93.73(10)	89.78(13), 90.32(12)	—
O(L1)–U–O(L1)	179.999(2)	74.37(8)	72.81(10)	80.0(6)
O(L1)–U–O(L2)	—	73.88(8)	69.36(11)	78.8(6)
O(L1)–U–O(L3)	—	—	—	91.6(4), 171.5(4)
O(L2)–U–O(L3)	—	—	—	172.4(4), 93.6(4)
O(L1)–U–X	90.1(3)	73.12(8), 146.82(8)	71.50(10), 144.17(11)	—
O(L2)–U–X	180.0	140.78(8), 68.94(8)	146.46(11), 72.89(10)	—

[a] L1 = Ph_3AsO (**2**), TPIP (**4**, **5** and **6**), L2 = Ph_3AsO (**2**), TPIP (**4**, **5** and **6**), X = Cl (**2**), O(thf) (**4**) and O(Cy_3PO) (**5**), L3 = bridging O(TPIP) (**6**).

trend is consistent with a synergic effect of axial and equatorial ligands on the uranyl bond strength. A red shift in the uranyl emission indicates a decrease in uranyl oxo bond order as a consequence of increased electron donation from the ancillary ligands (L) in the equatorial plane to the uranium centre. The observed lowering of the uranyl bond order as a function of donor strength is quite discernible, and mirrors the subtle changes observed in the crystal structures (Table 2), the Raman spectra and in the solution absorption spectra. Interestingly, these data suggest that the triphenyl phosphine oxide ligand is a stronger σ-donor than its triphenyl phosphinimine counterpart in this system. This is in contrast to competitive ligand displacement reactions and DFT calculations which suggest the contrary. However, these data do not take into account the relative amount of covalency in the bonding model which has been shown to be significant in the phosphinimine complex **3** as the experimental data include all bonding types.

The emission profiles of the uranyl LMCT bands in each complex additionally display some of the characteristic vibrational fine structure with either 3, 4 or 5 of the 'hot bands' being resolved; the higher energy vibronic bands are convoluted with the tail of the L→U LMCT emission (Fig. 2). Although the low resolution of the spectra precludes accurate determination of the vibronic progression that correspond to the ν_1 and ν_2 vibrational modes,[28,35] the spacings are comparable to the ν_1 Raman stretch (*e.g.* 833 cm^{-1} in **1**). The presence of vibrationally structured emission points to the fact that non-radiative back energy transfer quenching mechanisms to the aromatic electronic excited levels are not operative in these systems under ambient conditions as anticipated. The luminescence lifetimes of all the complexes were determined by time correlated single photon counting on the microsecond timescale following excitation at 405 nm with a pulsed picosecond diode laser in combination with a 450–550 nm bandpass interference filter to select the uranyl emission and exclude scattered light. The luminescence lifetimes of all the complexes (Table 1) vary dramatically with the nature of the ancillary ligand L. In uranyl halide systems, the halide ions efficiently quench the excited state uranyl through photoinduced electron transfer (PET).[29] Given that the number of halide ions in these systems are constant, additional quenching mechanisms that explain the observed differences in the luminescence lifetimes are likely to be bimolecular or vibrational in origin. In the parent compound $[UO_2Cl_2(thf)_2]_2$, the luminescence lifetime of 150 ns (corresponding to a rate constant of decay, k, of 6.67×10^6 s^{-1}) is particularly short for uranyl compounds. By comparison, the emission lifetime of $UO_2(NO_3)_2$ in H_2O is 1.0 μs at room temperature.[30,13] This short lifetime in $[UO_2Cl_2(thf)_2]_2$ can be explained by fast exchange of bound and free thf solvent molecules at ambient temperature, resulting in considerable bimolecular quenching. Accordingly, the kinetic decay profile of this compound was fitted to a biexponential decay, with a shorter-lived component (40 ns) convoluted with the longer-lived uranyl decay (150 ns); the contribution of the two components to the total luminescence intensity is approximately equal. The short (40 ns) component is assigned as radiative decay from the equatorial ligand-to-uranium LMCT. As the labile thf molecules are replaced by increasingly stronger donor moieties, the luminescence lifetimes of the 'yl' LMCT component of the emission increases, whereas the relative contribution of the L→U component decreases (*e.g.* to 7% in **3**, which is consistent with above findings). In particular, the uranyl LMCT lifetime is remarkably sensitive to the nature of the donor atoms in the primary coordination sphere and to vibrational deactivation. The heavier As atoms in **2** appears to suppress vibrational decay and increase the rate of intersystem crossing to the uranyl excited state, resulting in disappearance of the Ph_3AsO→U LMCT emission in the temporal profile and dramatically increasing the lifetime of the O_{yl}→U emission to 3.46 μs. Correspondingly, the rate of decay (k) decreases to 2.89×10^5 s^{-1}. In these complexes, the lengths of the luminescence lifetimes (μs) are sufficiently long to blur equatorial ligand exchange dynamics giving time averaged profiles.[31] Interestingly, the luminescence lifetimes of the uranyl emission follow the same trend as the shift in the emission maxima, providing an additional parameter with which to distinguish between members of a family of uranyl(VI) compounds based on their emissive properties.

Synthesis of uranyl(VI) tetraimidodiphosphinate (TPIP) complexes; 4–7

In light of the above, we extended our study to a related monoanionic bidentate ligand tetraphenylimidodiphosphine (TPIP) which is able to yield discrete multimetallic complexes with uranyl(VI)[32] and will enable us to correlate the number of uranyl units in a molecule with the emission profiles. The anion of TPIP, $[(Ph_2PO)_2N]^-$ possesses the correct electronic structure to render this study tractable, since the charge of the ligand is mainly localised on the amido nitrogen atom (*cf*. β-diketonates). The importance of using anionic ligands to probe the nature of the uranyl bond has been explored by numerous groups over recent years. Interestingly, the electronic properties of some of these ligands have been shown to cause activation of the O═U═O bond, perhaps most notably in the $\{UO_2\}^{2+}$ Lewis acid adduct $[UO_2(NCN)_2\{B(C_6F_5)_3\}]$ (NCN = $[PhC(NSiMe_3)_2]^-$), reported by Sarsfield *et al.* in 2004,[33] and in the uranyl(VI) complex of an expanded 'pacman' porphyrin prepared by Arnold and co-workers, which undergoes reductive *exo* oxo group silylation in the presence of a strong base such as $K[N(SiMe_3)_2]$.[34] The anion of tetraphenylimidophosphine $[(Ph_2PO)_2N]^-$ (TPIP) appears to promote the interesting and rather rare property of a $\{UO_2\}^{2+}$–$\{UO_2\}^{2+}$ uranium-oxo-uranium interaction in the trimetallic $[UO_2(TPIP)_2]_3$.[32] In this compound, the uranyl units are orthogonally connected *via* dative bonding of a Lewis basic uranyl oxygen to a neighbouring Lewis acidic metal centre (Scheme 2). These interactions can also be viewed as oxo bridges or 'cation–cation' interactions (*vide infra*) where the basicity of the oxo ligands may be a result of competition between the oxo ligands or charge repulsion of the uranyl units possessing different degrees of Lewis acidity.[35] The central O═U═O unit in the trimetallic framework bridges two uranyl(VI) ions through its 'yl' O atoms in a linear fashion of the type U···O═U═O···U. Additionally, Pikramenou *et al.* have demonstrated that this anion forms a hydrophobic shell when complexed to lanthanide(III) ions minimising vibrational quenching of inner and outer sphere solvent molecules.[36] We therefore sought to establish the optical properties of this trimeric complex and the possibility of forming lower order aggregates (monometallics, bimetallics) and investigate their solid state and solution forms.

Treatment of $UO_2Br_2{\cdot}3H_2O$ with Na[TPIP] in thf yields a monomeric thf adduct $[UO_2(TPIP)_2{\cdot}thf]$ (**4**). An analogous reaction in methanol followed by addition of tricyclohexyl phosphine oxide produces the phosphine oxide derivative (**5**). Both of these monomeric complexes were characterised in solution and in the solid state. Interestingly, repetition of the reaction described by Cea-Olivares *et al.*,[32] but by addition of Na[TPIP] to uranyl nitrate afforded, after isolation and recrystallisation, a previously unreported bimetallic complex $[UO_2(TPIP)_2]_2$ (**6**) and a small amount of the trimetallic complex $[UO_2(TPIP)_2]_3$ (**7**). Again, both of these complexes were characterised in the solid state and in solution. The $^{31}P\{^1H\}$ NMR spectra of this crude product mixture in CD_2Cl_2 displays two resonances at room temperature; a broad resonance at 25.9 ppm assigned to the trimetallic complex **7** by comparison with published data, and a singlet at 24.9 ppm, assigned to **6**. The relative ratios of the products **6** and **7** in this experiment are approximately 10 to 1 (as ascertained by ^{31}P NMR spectroscopy), and **6** can easily be isolated analytically pure by repeat recrystallisation to remove **7**. However, altering the stoichiometry of the reagents in the reaction has little effect on the product distribution; the trimetallic complex **7** is the only species that can be isolated at 1 : 1 and 2 : 1 ligand-to-metal ratios when uranyl nitrate is added to Na[TPIP]. Perhaps unsurprisingly, the addition of small polar molecules to **6** and **7**, results in dissociation of the aggregates into solvent stabilised monometallic products, so that dissolution of **6** and **7** in thf results in the formation of **4** and addition Cy_3PO in CH_2Cl_2 generates the phosphine oxide adduct **5**. It is apparent that in the absence of suitable polar molecules that occupy the 5th coordination site, the $\{UO_2\}^{2+}$–$\{UO_2\}^{2+}$ uranium-oxo-uranium interactions in **7** allow the U ions to retain the pentagonal bipyramidal geometry commonly seen in uranyl(VI) complexes and that this interaction is readily sacrificed in favour of binding to stronger Lewis bases.

X-ray crystal structures of the complexes 4, 5 and 6

Crystal structure of $[UO_2(TPIP)_2{\cdot}thf]{\cdot}thf$ (4). The complex $[UO_2(TPIP)_2{\cdot}thf]$ (**4**) crystallises with two structurally similar $\{UO_2\}^{2+}$ molecules and two disordered thf molecules contained in the asymmetric unit (Fig. 3). The central U atom of each uranyl complex exhibits a pentagonal bipyramidal coordination geometry, where each complex has two chelating TPIP groups. The first coordination sphere in each molecule is completed by a molecule of thf. Selected bond lengths and angles for the two molecules are given in Table 2. The two molecules of **4** have mean U═O bond distances that are statistically identical (U–O = 1.777(1) and 1.783(1) Å, respectively). The O═U═O angles

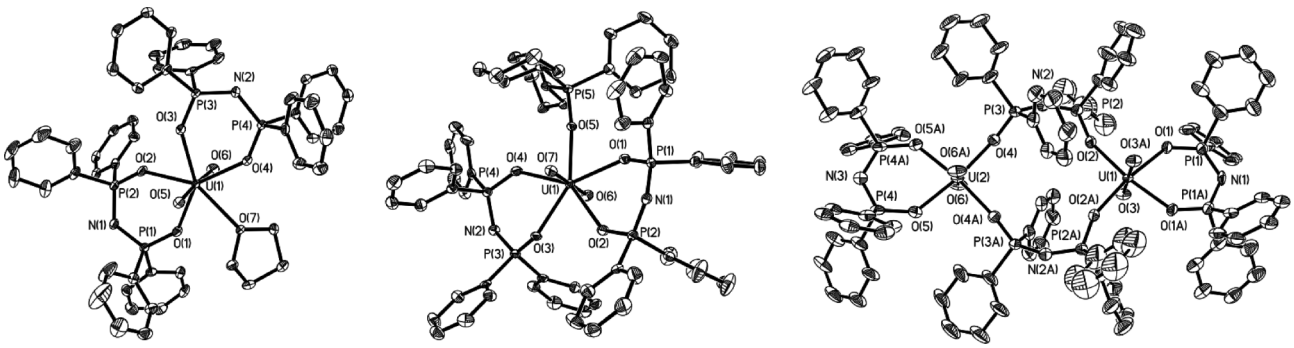

Fig. 3 Thermal ellipsoid plots of complexes **4** (left), **5** (middle) and **6** (right) at the 50% probability level; H atoms and lattice solvent molecules removed for clarity.

deviate slightly from linearity (176.0(1)° and 177.6(1)°) but still lie within the range reported for the majority of structurally characterised uranyl complexes. The average U–$O_{(TPIP)}$ distances measured (2.353(5) and 2.359(4) Å) are shorter than the values reported for the Th(IV) complex [Th(TPIP)$_4$] (2.41(3) Å) and in the analogous U(IV) homoleptic complex [U(TPIP)$_4$] (2.37(3) Å),[37] but are longer than in the seven-coordinate pentagonal bipyramidal complex [U(Cl)(TPIP)$_3$] (2.31(3) Å). The U–$O_{(THF)}$ distances of 2.504(2) Å and 2.516(2) Å compare well with the with the mean U–$O_{(THF)}$ bond length reported for the complex [$UO_2Br_2(THF)_3$], (2.46(3) Å).[38]

Crystal structure of [UO_2(TPIP)$_2$($OPCy_3$)] (5).1/2Et_2O. The phosphine oxide adduct, **5** is a monometallic charge neutral $\{UO_2\}^{2+}$ complex. Like the structure of **4**, the central uranium atom is seven-coordinate and ligated by two chelating monoanionic TPIP ligands. The pentagonal bipyramidal coordination geometry is completed by a monodentate P═O donor group (Cy_3PO). Selected bond lengths and angles are listed in Table 2.

The average U═O bond distance in **5** (1.771(2) Å) is shorter than that found for the $\{UO_2\}^{2+}$ group involved in the bridging interaction in [UO_2(TPIP)$_2$]$_3$ (1.793(4) Å), but significantly longer than the average terminal uranyl–oxo bond distance of 1.737(5) Å. The U–$O_{(TPIP)}$ distances in **5** span the range 2.367(3)–2.415(3) Å and are slightly longer than those measured in **4**. This difference is most likely due to the larger size of the fifth equatorially bound ligand (Cy_3PO) in comparison to thf in **4**.

Crystal structure of [UO_2(TPIP)$_2$]$_2$ (6)·3CH_2Cl_2. The asymmetric unit of **6** contains half the dimer, the other half being generated by 2-fold symmetry, with atoms U(1), U(2), N(1) and N(2) all lying on the same two-fold axis. The structure of **6** is rather unusual in that the complex is comprised of two structurally discrete uranyl ions (Fig. 3) which are four coordinate in the equatorial plane; d(U–U) = 7.141 Å. It can be envisaged as the precursor framework to **7**. The coordination geometry about each uranyl cation is best described as a distorted tetragonal bipyramid. In contrast to the solid state structure of **7**, the uranyl cations do not participate in any extra electrostatic interactions that would normally satisfy the coordination requirements of UO_2(VI) complexes of this ligand. The structure is a *pseudo* C_2-centrosymmetric dimer, where each uranyl cation is ligated by one terminal TPIP ligand and by two μ_2-bridging imidodiphosphinates. The mean terminal TPIP oxygen–uranyl distances are 2.275(8) Å (Table 2) and are shorter than those measured in **4** and **5**, but statistically indistinguishable from the mean bridging distances (2.252(8) Å). The coordination geometry of each uranium atom is best described as a distorted octahedron, where, the axial uranyl units are essentially linear; O(3)–U(1)–O(3A) 178.9(7)° and O(6)–U(1)–O(6A) 179.3(7)°, and the equatorial ligands form a distorted square plane (Table 2). The uranium coordination centres are not mutually co-planar and the dihedral angle between the mean square planes described by the TPIP ligand is 15.1° and that between the uranyl units is 14.0°. The uranium 'yl' oxo distances are as expected for discrete uranyl cations, each at 1.80(1) Å (for U(1)–O(3)) and (U(2)–O(6)).

Crystal structure of [UO2(TPIP)2]$_3$(7).0.5(C_6H_{14}). The 100 K crystal structure of **7** was determined (see ESI†) and established to be similar to the previously determined 293 K crystal structure,[32] except that half a hexane solvent molecule per trimer was found.

Vibrational analysis of the complexes 4–7

The $\{UO_2\}^{2+}$ ion possesses three characteristic vibrational stretching frequencies, which renders vibrational analysis a sensitive tool in assessing solid state uranyl bond strengths; the symmetric stretching frequency (ν_1), in the range 780–900 cm^{-1}, the asymmetric stretching frequency (ν_3), lying in the range 800–1000 cm^{-1}; and the bending vibration, appearing around the 200 cm^{-1} region.[39]

The Raman active symmetric stretches (ν_1) for **4** and **5** are 840 and 827 cm^{-1}, respectively. These values are lower than the average ν_1 for the uranyl group (~860 cm^{-1}),[40] which may reflect a slight lengthening of the uranyl bond as a consequence of increased competition for overlap of the σ and π orbitals of the TPIP O atoms with the 5f bonding orbitals. For comparison, the Raman spectrum of [UO_2(TPIP)$_2$]$_3$ (**7**) was recorded.† The spectrum is very informative and confirms the presence of two distinct $\{UO_2\}^{2+}$ symmetric stretching frequencies (ν_1) (834 and 819 cm^{-1}). It is useful to consider the $\{UO_2\}^{2+}$–alkoxide tetrametallic species [UO_2(OCH(^{i}Pr)$_2$)$_2$]$_4$ isolated by Wilkerson *et al.*[35] when assigning the bands in this spectrum. This compound exhibits a bent UO_2→U dative bond and displays the lowest reported ν_1 value (713 cm^{-1}) of any $\{UO_2\}^{2+}$ complex to date. The large reduction in the ν_1 stretching frequency of the O═U═O unit in [UO_2(OCH(^{i}Pr)$_2$)$_2$]$_4$ was considered to be more greatly influenced by its coordination to a neighbouring Lewis acid than by coordination of strongly donating ligands in the equatorial plane. Accordingly, the band at lower energy (819 cm^{-1}) in the Raman spectrum of [UO_2(TPIP)$_2$]$_3$ (**7**) is assigned as the O═U═O unit involved in the O···O═U═O···O bridging interaction, whilst the band at higher energy (834 cm^{-1}) is likely to arise from the stronger U═O bonds of the two terminal $\{UO_2\}^{2+}$ moieties in [UO_2(TPIP)$_2$]$_3$.

Solution structures of the complexes

Multinuclear NMR spectroscopic studies. At 298 K compounds **4** and **5** both exhibit a broad singlet in their $^{31}P\{^1H\}$ NMR spectra (CD_2Cl_2) attributable to the complexed TPIP groups at 24.2 and 24.7 ppm respectively.† The phosphine oxide adduct **5** additionally displays a resonance at 64.9 ppm. A low temperature study reveals that at 268 K, this resonance in **5**, can be separated into two individual components at δ 24.8 and 23.6 ppm corresponding to the two magnetically inequivalent ^{31}P atoms of the TPIP ligands as seen in the solid state structure. A similar variable temperature NMR spectroscopic study of **4** reveals that no exchange processes can be frozen out at low temperature within the temperature limits of the solvent by $^{31}P\{^1H\}$ NMR spectroscopy. However, the thf spectral resonances in the ^1H experiment do resolve into two sets at 201 K. This indicates that exchange of bound and free thf is slow on the NMR timescale at low temperature and conversely, fast at room temperature.

In contrast to the trimetallic complex [UO_2(TPIP)$_2$]$_3$ (**7**), whose $^{31}P\{^1H\}$ spectra are broad at 298 K and separate into three distinguishable peaks at 233 K,[32] the dimetallic complex [UO_2(TPIP)$_2$]$_2$ (**6**), exhibits sharp $^{31}P\{^1H\}$ and ^1H NMR spectra down to 213 K. This indicates that the TPIP ligands in the dimetallic form are conformationally much less rigid than in the trimer **7**, where the $\{UO_2\}^{2+}$–$\{UO_2\}^{2+}$ uranium–oxo–uranium interactions impart a higher degree of rigidity upon the complex.

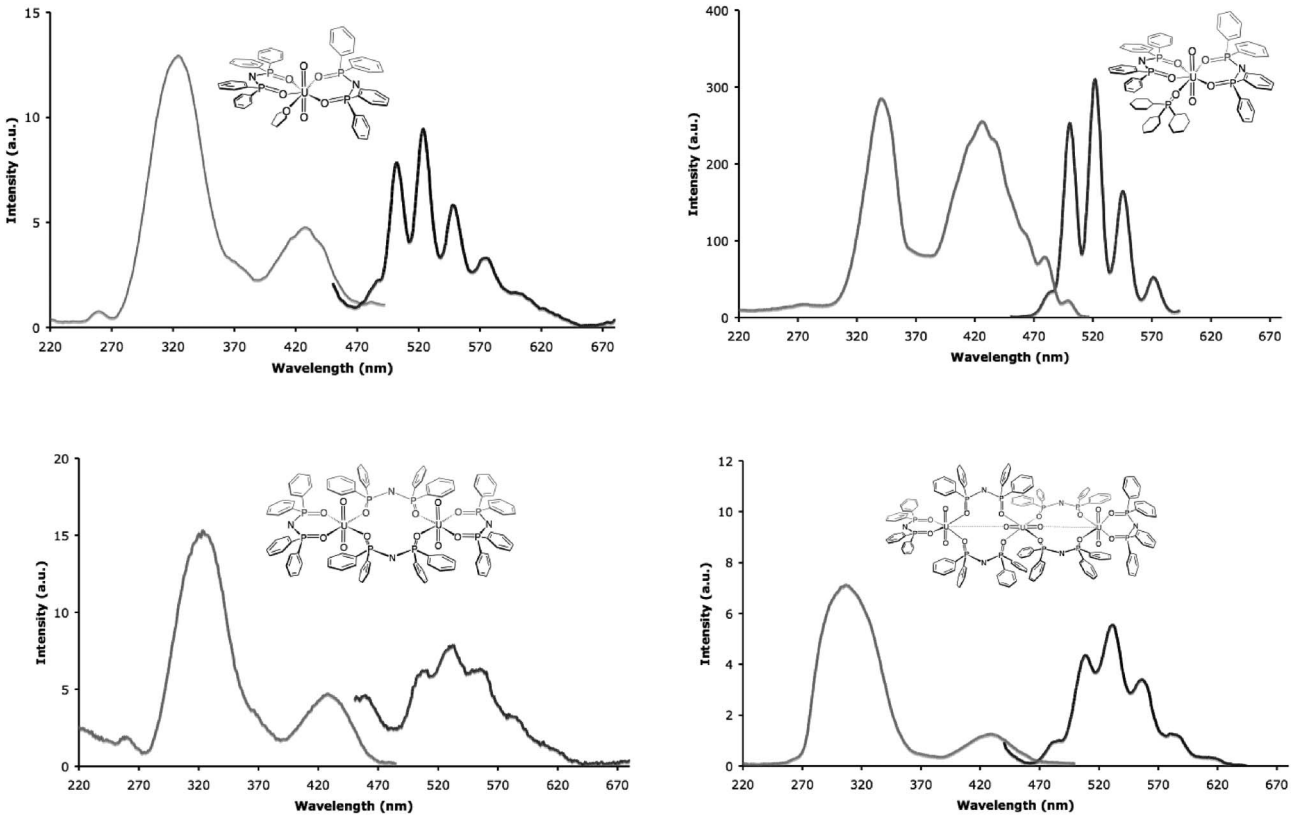

Fig. 4 Corrected steady state emission following excitation at 420 nm (295 K), (black traces) and excitation spectra (grey traces) of **4–7** in air equilibrated CH_2Cl_2. The emission centered at *ca.* at 420 nm is assigned as the equatorial donor to uranium LMCT and the emission centered at *ca.* 520 nm is the uranyl U═O LMCT emission. The spectral profiles are similar following 360, 375 and 405 nm excitation.

Photophysical properties of the complexes 4–7. The ground state electronic absorption spectra of the complexes were recorded in CH_2Cl_2 solutions; the principal absorption maxima are listed in Table 1 and the excitation and emission spectra are shown in Fig. 4. The spectra of all the complexes display two intense broad transitions in the UV region (between 200 and 350 nm) which are assigned to spin allowed, ligand centred (LC) $^1\pi$–π^* transitions and TPIP O→U LMCT transitions as observed in the compounds **1–3**. In addition to these ligand based transitions, the weaker Laporte disallowed $O_{yl'}$→U absorption is observed at *ca.* 425 nm evidencing the associated well resolved vibronic fine structure (~ 12 lines).

Following excitation into each one of the absorption bands (260–460 nm) the luminescence spectra that result are dominated by the uranyl $O_{yl'}$→U emission bands, superimposed upon which are 6 vibronic bands. As with the $[UO_2Cl_2(L_2)]$ series (**1–3**), the uranyl emission is also convoluted with the TPIP O→U LMCT band at higher energy (~ 400 nm) in the fluorescence spectrum. Notably, the apparent $E_{0\text{-}0}$ transitions and the maxima of the 'yl' LMCT emission are comparable for the iso-symmetric complexes **4** and **5** ($E_{0\text{-}0}$ = 19 920 cm^{-1} and 20 040 cm^{-1} respectively) and it is evident that replacement of thf for Cy_3PO has a small influence on the uranyl bonding as observed with analogues bearing monodentate donors **1–3**. The form of the emission spectra are also rather informative and evidence the different degrees of vibrational interactions between these complexes. The individual vibronic bands in **4** are broader than those in **5** as a consequence of rapid exchange of the thf ligand in solution (as observed by NMR spectroscopy). Despite this, the average progressional spacings in both complexes of 837 cm^{-1} (**4**) and 843 cm^{-1} (**5**) are in close agreement with the experimentally determined ν_1 asymmetric modes. By contrast, there are fewer vibrational features in the $[UO_2Cl_2(L_2)]$ series than in the monometallic complexes **4** and **5**; an observation most likely attributable to the increased lability of the neutral monodentate donors with respect to the anionic bidentate TPIP ligands.

By comparison with the monometallic complexes **1–5**, the dimetallic complex **6** and the trimetallic complex **7**, display apparent $E_{0\text{-}0}$ transitions and emission maxima at considerably lower energy ($E_{0\text{-}0}$ = 19 670 cm^{-1} and 19 650 cm^{-1} respectively). In the latter, the presence of uranyl Lewis acid–base interactions and a concomitant elongation of the uranyl bonds can explain this shift to lower energy[35] but in the bimetallic **6**, these interactions are absent since the intermetallic uranium distance is long at 7.141 Å. For comparison, the intermetallic separations between the central and terminal U ions in **7** are 4.352 and 4.397 Å. The apparent red shift in the luminescence profile in **6**, therefore may be a result of coordinative unsaturation at the metal centre so that the equatorial TPIP ligands compensate the charge on the uranyl cation by engaging in stronger electrostatic interactions, accordingly shortening the TPIP O–U bond distance and lengthening the uranyl bonds (as observed by X-ray crystallography).

Interestingly, in the bimetallic **6**, the emission spectra are considerably further broadened than in **4** and **5**, illustrating the

enhanced conformational freedom of the bridging ligands of this complex in solution (also observed by NMR spectroscopy). However, in the trimetallic, **7**, where the structure remains intact in solution, the vibrational bands are resolved but less so than in the monometallic analogue **5**. The vibrational spacings of the four most intense bands in the trimetallic complex **7** of 849, 827 and 758 cm^{-1} (average = 811 cm^{-1}) are clearly smaller than in monometallic complexes, which have similar progressional spacings (average of 837 cm^{-1} for **4** and 843 cm^{-1} for **5**), indicating that one or more uranyl bond distances exist in the ground state. Coupled with the fact that the emission maximum is observed at lower energy, this suggests that in the excited state, the uranyl bonds are significantly elongated. It seems plausible that a range of $U–O_{yl}$ distances may exist in the excited state and/or that this state is partially delocalised across several U centres. Indeed, in the lower energy vibronic bands, there appears to be two components to the emission envelope, suggesting that the excited state complex possesses more than one structurally distinct uranyl environment.

The luminescence lifetimes of the complexes further corroborate these findings; the luminescence lifetime of the trimetallic **7** of 1.04 μs is reduced to approximately half of that of the monometallic analogue **5** (2.00 μs), in which the uranyl cation is essentially vibrationally isolated. The associated rate constants for decay are 9.62×10^5 s^{-1} (**7**) and 5.00×10^5 s^{-1} (**5**). The increased rate of luminescence decay in **7** indicates that an intermetallic vibronic process between the orthogonally connected uranyl units in the excited state is probably responsible for this quenching. By contrast, the rate constants of excited state deactivation in the bimetallic complex **6** and the monometallic thf adduct **4**, (respectively, 9.23×10^5 s^{-1} and 1.67×10^6 s^{-1}) are approximately an order of magnitude greater than phosphine oxide adduct **5** (5.00×10^5 s^{-1}) as a result of vibrational and collisional deactivation of the excited state uranyl ions since the uranyl cations in these systems are well isolated. The temporal decay profiles in all the TPIP complexes (450–550 nm) fitted well to monoexponential kinetics; the contribution of the secondary TPIP O→U LMCT emission being < 1% and as with the complexes **1–3**, the TPIP O→U LMCT is able to sensitise the O_{yl}→LMCT emission quite effectively when excited at shorter wavelengths. The quantum yields of luminescence (measured relative to quinine sulfate) are all less than 0.5%, but suggest that vibrational and collisional quenching due to ligand vibrations and solvent exchange in **4** and **6** is more effective at reducing the number of photons emitted than the intermetallic quenching mechanism in **7**, which is a much more rigid structure in solution on the timescale of the luminescence experiment.

Conclusions

Two families of uranyl complexes bearing monodentate and bidentate ligands that are structurally relevant to nuclear fuel reprocessing cycles have been prepared and fully characterised. Limiting the absorption envelope of the chromophoric groups in the ligands to the UV gives rise to strongly emissive compounds in fluid solution at room temperature by inhibiting competitive back energy transfer processes from the emissive uranyl LMCT state. In the series of complexes bearing monodentate Ph_3PO, Ph_3AsO and Ph_3PNH ligands (**1–3** $[UO_2Cl_2(L)_2]$), the steady state and temporal emission profiles are extremely sensitive to the electronic environment around the uranyl ion and to vibrational deactivation, providing a good probe of the equatorial ligand to uranyl donor strength and relative basicity of the uranyl oxo group. The monoanionic bidentate ligand tetraphenylimidodiphosphinate (TPIP) reacts with uranyl(VI) precursors to yield discrete monometallic, bimetallic and trimetallic complexes $[UO_2(TPIP)(thf)]$ (**4**), $[UO_2(TPIP)(Cy_3PO)]$ (**5**), $[UO_2(TPIP)_2]_2$ (**6**) and $[UO_2(TPIP)_2]_3$ (**7**). The trimetallic is rather unusual since the central uranyl ion is orthogonally connected to two peripheral ones *via* uranyl → uranium dative bonds or 'cation–cation' interactions; these interactions appear to persist in solution in addition to the solid state. Each complex displays a unique luminescent fingerprint; the emission maxima, spectral shape and emission lifetimes are characteristic for each. In, the bimetallic **6**, the two uranyl cations are well isolated and essentially behave as independent uranyl units. However, in **7**, the close uranyl–uranyl contacts result in considerable excited state intermetallic quenching reducing the luminescence lifetime by approximately a factor of two. This study demonstrates that time resolved and multi-parametric luminescence can be of value in ascertaining solution and structural forms of well defined uranyl(VI) complexes in non-aqueous media.

Experimental

General details

All chemical reagents were obtained from the Aldrich Chemical Company and were used as supplied or recrystallised before use. The compounds $[UO_2Cl_2(thf)_2]_2$,[23] $[UO_2Cl_2(Ph_3PO)_2]$ (**1**),[25] $[UO_2Cl_2(Ph_3PNH)_2]$ (**3**)[24] and Na[TPIP][43] were prepared according to literature procedures. Uranium trioxide UO_3 was obtained from the Centre for Radiochemistry Research (CRR) isotopes store at The University of Manchester. ***Caution! Natural uranium was used during the course of these experiments. As well as the radiological hazards, uranium is a toxic metal and care should be taken with all manipulations. Experiments using uranium materials were carried out using pre-set radiological safety precautions in accordance with the local rules of The University of Manchester.***

Reagent grade thf and hexane were dried over potassium/benzophenone and CH_2Cl_2 from CaH_2 and all solvents were distilled and degassed prior to use. Deuterated CD_2Cl_2 was dried over CaH_2 and vacuum transferred and thoroughly degassed before use. Air sensitive experiments were performed standard Schlenk techniques and subsequent manipulation of materials were conducted in an argon filled Saffron glove box equipped with O_2 and H_2O analysers.

All NMR spectra were recorded on a Bruker Avance 400 spectrometer, operating frequency 400 MHz (^1H), 100 MHz (^{13}C) and 162 MHz ($^{31}P\{^1H\}$) variable temperature unit set at 295 K, unless otherwise stated. Chemical shifts are reported in parts per million relative to TMS (^1H) or H_3PO_4 ($^{31}P\{^1H\}$) and referenced to the residual proton resonances in CD_2Cl_2.

Raman and infrared spectroscopy experiments of uranium-containing samples were performed on a Bruker Equinox 55 FTIR/Raman machine equipped with a "Golden Gate" ATR (Attenuated Total Reflectance) attachment (resolution 4 cm^{-1}). Solid state Raman spectra were recorded by preparing each sample

Table 3 Data collection and structural refinement for complexes **2**, **4**, **5** and **6**

Complex	**2**	**4**	**5**	**6**
Empirical formula	C_{36} H_{30} As_2 Cl_2 O_4 U, $2(CH_2Cl_2)$	C_{52} H_{48} N_2 O_7 P_4 U, C_4 H_8 O	C_{66} H_{73} N_2 O_7 P_5 U, $0.5(C_4H_{10}O)$	C_{96} H_{80} N_4 O_{12} P_8 U_2, $3(CH_2Cl_2)$
Formula weight	1155.22	1246.94	1436.20	2460.24
T/K	100(2)	100(2)	100(2)	100(2)
Wavelength/Å	0.71073	0.71069	0.71069	0.71073
Crystal system, space group	Monoclinic, $P2_1/n$	Triclinic, $P\bar{1}$	Triclinic, $P\bar{1}$	Monoclinic, $C2/c$
a, b, c/Å	9.736(5), 15.284(5), 14.026(5)	12.469(5), 16.035(5), 26.736(5)	9.849(5), 13.004(5), 26.892(5)	21.980(5), 27.412(6), 17.356(4)
α, β, γ (°)	90, 101.671(5), 90	89.730(5), 78.123(5), 85.965(5)	96.380(5), 92.738(5), 110.122(5)	90, 101.420(5), 90
Volume/Å^3	2044.0(14)	5218(3)	3200(2)	10250(4)
Z	2	4	2	4
Density (calculated)/Mg m^{-3}	1.877	1.587	1.490	1.594
Absorption coefficient/mm^{-1}	6.007	3.290	2.716	3.497
Crystal form, colour	Prismatic, yellow	Irregular, yellow	Plate, yellow	Needle, colourless
Crystal size/mm^3	$0.15 \times 0.15 \times 0.15$	$0.30 \times 0.30 \times 0.20$	$0.25 \times 0.20 \times 0.10$	$0.30 \times 0.10 \times 0.05$
Theta range for data collection (°)	1.99 to 24.38	1.49 to 26.41	1.68 to 26.38	1.82 to 23.26
Index ranges	$-11 \le h \le 11$, $-17 \le k \le 17$, $-16 \le l \le 16$	$-15 \le h \le 15$, $-19 \le k \le 20$, $-33 \le l \le 33$	$-12 \le h \le 12$, $-16 \le k \le 16$, $-33 \le l \le 33$	$-24 \le h \le 24$, $-30 \le k \le 30$, $-19 \le l \le 19$
No. of measured, independent, observed reflections ($I > 2\sigma(I)$)	13062, 3273, 2277	42041, 21104, 18196	25835, 12910, 11156	31354, 7364, 3725
R(int)	0.135	0.0271	0.0448	0.2237
Absorption correction	Semi-empirical from equivalents	Semi-empirical from equivalents	Semi-empirical from equivalents	None
T_{max}, T_{min}	0.6450, 0.3796	1.000, 0.669	1.000, 0.733	
Refinement method	Full-matrix least-squares on F^2	Full-matrix least-squares on F^2	Full-matrix least-squares on F^2	Full-matrix least-squares on F^2
Data/restraints/parameters	3273/0/232	21104/0/1274	12910/0/757	7364/574/519
$R[F^2 > 2\sigma(F^2)]$, $wR(F^2)$, S	0.0728, 0.2039, 1.007	0.0316, 0.0828, 1.033	0.0442, 0.0903, 1.031	0.0764, 0.1511, 0.885
$\Delta\rho_{max}$, $\Delta\rho_{min}$/e Å^{-3}	3.047, –3.218	2.649, –1.339	1.534, –1.264	1.097, –1.905

in a glass capillary, sealing the capillary with "Blue-Tac" and then fixing the sample in the path of the laser beam for up to 5 h.

Elemental analyses on uranium-containing samples were performed by M. Jennings and colleagues in the microanalytical laboratory in the School of Chemistry at the University of Manchester. A Carlo ERBA Instruments CHNS–O EA1108 elemental analyzer was used for C, H and N analysis and a Fisons Horizon elemental analysis ICP-OED spectrometer for U, P, and halides.

X-ray diffraction data for **2**, **4**, **5**, **6** and **7** were collected at 100 K using a Bruker AXS SMART diffractometer using graphite-monochromated Mo-Kα radiation. Data were corrected for Lorentz and polarisation factors and absorption corrections were applied using Bruker SADABS. Crystal data, data collection and structural refinement parameters are given in Table 3. The structures were solved by direct methods using the program SHELXS-97.[44] Full matrix refinement on F^2 and all further calculations were performed using SHELXL-97 and the SHELXTL package. The non-H atoms were refined anisotropically, except for the disordered thf solvent atoms in **4**. Hydrogen atoms were positioned in idealised sites and were allowed to ride on their parent C or N atoms; those bonded to the disordered Et_2O molecule in **5** were omitted The structures contained a number of disordered solvent molecules which were modelled by parts with some restraints on the geometry.

Photophysical characterisation

Absorption spectra were recorded in CH_2Cl_2 on a T60U spectrometer (PG Instruments Ltd.) using fused quartz cells with a path length of 1 cm or on a on a double-beam Cary Varian 500 scan UV–vis–nIR spectrophotometer over the range 300–1300 nm.

Steady state emission and excitation spectra were determined using a Perkin-Elmer LS55 fluorimeter operating in fluorescence mode or a Perkin-Elmer LS50 B fluorimeter operating in fluorescence mode. The spectra were corrected for both the excitation source and the emission spectral response. Time resolved luminescence measurements were recorded using an Edinburgh instruments mini-Tau system by time correlated single photon counting using an EPL 375 or EPL 405 picosecond diode laser as the excitation source. Lifetimes were obtained by tail fit on the data obtained, and quality of fit judged by minimization of reduced χ^2 and residuals squared.

The quantum yields of luminescence of the complexes were determined in CH_2Cl_2 solutions relative to quinine sulfate in 0.1 M H_2SO_4 which has a known quantum yield of 58% at 350 nm excitation at 295 K. The details of this approach have been described in detail elsewhere.[45]

Preparation of *trans*-$[UO_2Cl_2(Ph_3AsO)_2]\cdot 2CH_2Cl_2$ (2)

Under Ar, a solution of Ph_3AsO (0.27 g, 0.82 mmol) in thf was added dropwise to a thf solution of $[UO_2Cl_2(thf)_2]_2$ (0.20 g, 0.4 mmol). A pale yellow precipitate formed immediately. The resulting mixture was stirred for 2 h and the precipitate was filtered, washed with thf (2 ×10 ml) and dried under vacuum to yield a pale yellow solid. Crystals were obtained from slow evaporation of a concentrated solution of **2** in CH_2Cl_2. Yield 0.23 g, 58.5%. ^{1}H NMR (CD_2Cl_2): δ (ppm) 7.4–8.1 (m, C*H*-Ph). Anal. Calcd for

$C_{36}H_{30}O_4As_2Cl_2U{\cdot}0.75CH_2Cl_2$: C, 42.07; H, 3.03; N, 0.00. Found: C, 42.29; H, 2.62; N, 0.00.

Preparation of uranyl bromide hydrate, $UO_2Br_2{\cdot}xH_2O$

UO_3 (7.93 g, 27.73 mmol) was dissolved in 48% HBr (50 mL) to give a deep orange solution. The volume was reduced (*ca.* 5 mL) by heating, giving an orange–red solution. Further 48% HBr (2 × 5 mL) was added and the volume again reduced (*ca.* 5 mL). The solution was evaporated to dryness *in vacuo* and the resulting residue dissolved in warm de-ionised water (50 mL). The yellow solution was reduced in volume (*ca.* 5 mL) by heating, yielding a deep orange solution, which was evaporated to dryness *in vacuo* and the resulting orange residue $UO_2Br_2{\cdot}xH_2O$, was dried at 100° C under vacuum overnight. Yield: 10.11 g, 81%. Anal. Calcd for $Br_2H_{3.5}O_{3.75}U$: Br, 34.64; H, 0.38; N, 0.00; U, 51.59. Found: Br, 33.96; H, 0.58; N, 0.00; U, 51.44.

Preparation of $[UO_2(TPIP)_2(thf)]{\cdot}thf$ (4)

Under Ar, $UO_2Br_2{\cdot}3H_2O$ (0.30 g, 0.62 mmol) was dissolved in thf (15 mL). A solution of Na[TPIP] (0.54 g, 1.24 mmol) in thf (10 mL) was slowly added with stirring. A white precipitate (NaBr) immediately developed. The reaction mixture was stirred at ambient temperature for 10 min and then centrifuged for 3 m (3000 rpm) in air and filtered. The volume of the filtrate was reduced to *ca.* 5 mL and then transferred to two small vials. Diffusion of diethyl ether vapour into the concentrated thf solutions produced luminous green–yellow crystals overnight. The vials were left undisturbed for a further 2 d and the crystals collected by filtration, washed with Et_2O (15 mL) and air dried. Yield 0.46 g, 63%. $^{31}P\{^1H\}$ NMR (CD_2Cl_2): δ (ppm) 24.69 (br). ^1H NMR (CD_2Cl_2): δ (ppm) 1.4 (m, 4H, C*H*$_2$–thf), 4.1 (m, 4H, C*H*$_2$–thf), 7.0–8.1 (m, 40 H, C*H*–Ph). Anal. Calcd for $C_{52}H_{48}N_2O_7P_4U$: C, 53.15; H, 4.09; N, 2.39; P, 10.56; U, 20.27. Found: C, 52.52; H, 4.04; N, 2.30; P, 10.45; U, 20.10. IR (4000–500 cm^{-1}, solid sample on ATR cell): 3049(w), 2987(w), 2889(w), 1591(w), 1482(w), 1436(m), 1310(w), 1286(w), 1211(m), 1179(sh), 1122(s), 1078(s), 1056(s), 1023(s), 997(m), 916(s), 879(m), 823(m), 750(m), 724(m), 692(s), 618(m), 585(m), 549(m), 534(sh), 512(s); Raman (solid in glass capillary, 3500–500 cm^{-1}): 3145(w), 3054(s, br), 3010(w), 2988(w), 2894(w), 1592(m), 1574(sh), 1183(w), 1158(w), 1029(w), 1000(s), **O═U═O$_{(symm)}$840(m)**, 692(w), 618(w).

Preparation of $[UO_2(TPIP)_2(OPCy_3)]{\cdot}1/2Et_2O$ (5)

$UO_2Br_2{\cdot}3H_2O$ (0.35 g, 0.72 mmol) was dissolved in MeOH (15 mL). A solution of Na[TPIP] (0.63 g, 1.44 mmol) in MeOH (15 mL) was slowly added with stirring. A pale yellow–green precipitate immediately developed, the reaction mixture was stirred for a further 3 h. The precipitate was collected by filtration and washed with MeOH (2 × 5 mL). The solid was dissolved in thf (10 mL), centrifuged for 3 min (3000 rpm) and the solution filtered to remove the NaBr byproduct. A solution of Cy_3PO (0.21 g, 0.72 mmol) in thf (4 mL) was added slowly with stirring and the reaction mixture covered and left to stir overnight. The reaction mixture was slowly poured over Et_2O (100 mL), which was being vigorously stirred and was then left to stand undisturbed. After 5 h a large mass of luminous yellow–green crystals had formed, the liquor was decanted away and the crystals air dried and then dried *in vacuo* overnight. Yield 0.41 g, 41%. $^{31}P\{^1H\}$ NMR (CD_2Cl_2): δ (ppm) 64.92 (s), 24.17 (br). ^1H NMR (CD_2Cl_2): δ (ppm) 0.7–2.2 (m, 33H, C*H*–Cy, C*H*$_3$–Et$_2$O), 3.3 (q, 2H, C*H*$_2$–Et$_2$O), 7.0–8.1 (m, 40H, C*H*–Ph). Anal. Calcd for $C_{68}H_{78}N_2O_{7.5}P_5U$: C, 56.86; H, 5.44; N, 1.92; P, 10.80; U, 16.59. Found: C, 56.51; H, 5.28; N, 1.95; P, 11.14; U, 16.86. IR (4000–500 cm^{-1}, solid sample on ATR cell): 3056(w), 2928(w), 2853(w), 1592(w), 1483(w), 1437(m), 1163(m), 1123(s), 1091(s), 1065(s), 1027(m), 998(m), 911(s), 851(m), 828(m), 751(m), 723(s), 693(s), 588(m), 551(s), 515(s); Raman (solid in glass capillary, 3500–500 cm^{-1}): 3146(w), 3058(s), 3011(m), 2942(s), 2861(s), 1592(m), 1575(sh), 1443(w), 1292(w), 1170(w), 1120(w), 1030(m), 1000(s) **O═U═O$_{(symm)}$827(m)**, 696(m), 618(w).

Preparation of $[UO_2(TPIP)_2]_2{\cdot}3CH_2Cl_2$ (6)

According to a slight modification of a literature procedure,[32] 0.145 g of Na[TPIP] (0.33 mmol) was dissolved in 5 mL of ethanol and added to a solution of 0.086 g (0.17 mmol) $UO_2(NO_3)_2{\cdot}6H_2O$ in 5 mL of deionised water, producing a cloudy green colour. After an hour, the solution was filtered to leave a yellow precipitate which was left to dry in air overnight. The precipitate was then dissolved in 2 mL of CH_2Cl_2 and layered with 10 mL of n-hexane and left to crystallise. Both pale yellow/colourless needles (**6**) and yellow plates (**7**) suitable for X-ray diffraction were collected from the side of the vial after 4 d. The crystalline material was isolated and slow evaporation of the supernatant afforded a yellow powder of **6** in 37% yield (0.07 g).

$^{31}P\{^1H\}$ NMR (CD_2Cl_2): δ (ppm) 24.92 (s). ^1H NMR (CD_2Cl_2): δ (ppm) 7.95 (m, 3H, C*H*-Ph), 7.26 (m, 2*H*, CH-Ph). Anal. Calcd for $C_{96}H_{80}N_4O_{12}P_8U_2.C_6H_{14}$: C, 53.46; H, 4.13; N, 2.44; P, 10.81; U, 20.77. Found: C, 53.31; H, 3.83; N, 2.41; P, 10.91; U, 21.06. IR (4000–500 cm^{-1}, solid sample on ATR cell): 1436(m), 1203(w), 1121(m), 1022(m), 914(s), 797(m), 747(m), 722(s), 689(s), 586(s), 549(s), 507(s).

Preparation of $[UO_2(TPIP)_2]_3.0.5(C_6H_{14})$ (7)

According to a slight modification of the literature procedure,[32] 0.165 g $UO_2(NO_3)_2{\cdot}6H_2O$ (0.33 mmol) in H_2O (5 mL) was added to a solution of Na(TPIP) (0.145 g, 0.33 mmol) in ethanol (5 mL). The solution was stirred for one hour and the yellow precipitate was filtered and dissolved in 2 mL CH_2Cl_2 followed by the addition of 10 mL n-hexane. The yellow plates that crystallised were isolated by filtration and characterised. Analytical data of the isolated product were consistent with published data for **7**.

$^{31}P\{^1H\}$ NMR (CD_2Cl_2): δ (ppm) 25.92 (s). ^1H NMR (CD_2Cl_2): δ (ppm) 8.12 (m, 2H, C*H*-Ph), 7.32 (m, 3H, C*H*-Ph). Raman (solid in glass capillary, 1200–500 cm^{-1}): 1185(w), 1150(m), 1123(m), 1040(m), 998(s) **O═U═O$_{(symm)}$834(m)**, **819(m)**, 694(m), 617(m).

Acknowledgements

We thank the EPSRC for funding a Career Acceleration Fellowship (LSN), for provision of a postdoctoral grant GR/595152/01 (SMC) a studentship (SDW) and a Nuclear 1st DTC studentship (DW). We also thank Dr Clint Sharrad for his assistance with crystal structure of **2** and Dr Daniel Sykes and Prof. Stephen Faulkner for help with the luminescence measurements of the complexes and for helpful discussions.

Notes and references

1 See for example:L. R. Avens, S. G. Bott, D. L. Clark, A. P. Sattelberger, J. G. Watkin and B. D. Zwick, *Inorg. Chem.*, 1994, **33**, 2248; J. C. Berthet, M. Nierlich and M. Ephritikhine, *Chem. Commun.*, 2004, 870; J. C. Berthet, M. Nierlich and M. Ephritikhine, *Dalton Trans.*, 2004, 2814; L. Natrajan, M. Mazzanti, J.-P. Bezombes and J. Pécaut, *Inorg. Chem.*, 2005, **44**, 6115; L. Natrajan, F. Burdet, J. Pécaut and M. Mazzanti, *J. Am. Chem. Soc.*, 2006, **128**, 7152; J. C. Berthet, G. Siffredi, P. Thuéry and M. Ephritikhine, *Chem. Commun.*, 2006, 3184; C. D. Carmichael, N. A. Jones and P. L. Arnold, *Inorg. Chem.*, 2008, **47**, 8577; J. C. Berthet, P. Thuéry and M. Ephritikhine, *Inorg. Chem.*, 2005, **44**, 1142; A. E. Enriguez, B. L. Scott and M. P. Neu, *Inorg. Chem.*, 2005, **44**, 7403; T. W. Hayton, J. M. Boncella, B. L. Scott, E. R. Batista and P. J. Hay, *J. Am. Chem. Soc.*, 2006, **128**, 10549.

2 *'Meeting the Energy Challenge, A White Paper on Energy'*, Department of Trade and Industry, May 2007, Crown Copyright, 2007*Meeting the Energy Challenge, A White Paper on Energy'*, Department of Trade and Industry, January 2008, Crown Copyright, 2008.

3 G. G. Stokes, *Phil. Trans. Roy. Soc. London*, 1852, **142**, 518.

4 E. Gaillou, A. Delaunay, B. Rondeau, M. Bouhnik-le-Coz, E. Fritsch, G. Cornen and C. Monnier, *Ore Geol. Rev.*, 2008, **34**, 113.

5 Y. Sugitani, K. Kato and K. Nagashima, *Bull. Chem. Soc. Jpn.*, 1979, **52**, 918.

6 S. L. Suib and K. A. Carrado, *Inorg. Chem.*, 1985, **24**, 200; A. L. Locock and P. C. Burns, *J. Solid State Chem.*, 2004, **177**, 2675; A. G. D. Nelson, T. H. Bray, W. Zhan, R. G. Haire, T. S. Sayler and T. E. Albrecht-Schmitt, *Inorg. Chem.*, 2008, **47**, 4945.

7 E. Rabinowitch, R. L. Bedford, *Spectroscopy and Photochemistry of Uranyl Compounds*, Pergamon Press, Oxford, 1964, 112.

8 V. V. Syt'ko and D. S. Umreiko, *J. Appl. Spectrosc.*, 1998, **65**, 857; K. Ohwada, *Spectrochim. Acta*, 1978, **35A**, 99.

9 G. Meinrath, *Freiburg On-line Geoscience*, 1998, **1**, 1; C. K. Jorgensen and R. Reisfeld, *Struct. Bonding*, 1982, **50**, 122(Heidelberg); J. L. Sessler, P. Melfi and G. D. Pantos, *Coord. Chem. Rev.*, 2006, **250**, 816; R. Ghosh, J. A. Mondal, H. N. Gosh and D. K. Palit, *J. Phys. Chem. A*, 2010, **114**, 5263.

10 R. G. Denning, *Structure and Bonding*, 1992, **79**, 215(Berlin); J. R. Plaisier, D. J. W. IJdo, C. de Mello Donega and G. Blasse, *Chem. Mater.*, 1995, **7**, 738; R. G. Denning, *J. Lumin.*, 2008, **128**, 1745.

11 J. T. Bell and R. Biggers, *J. Mol. Spectrosc.*, 1965, **18**, 247; J. T. Bell and R. Biggers, *J. Mol. Spectrosc.*, 1968, **25**, 312; S. P. McGlynn and J. K. Smith, *J. Mol. Spectrosc.*, 1961, **6**, 164.

12 R. G. Denning, *J. Phys. Chem. A*, 2007, **111**, 4125; F. Réal, V. Vallet, C. Marian and U. Wahlgren, *J. Phys. Chem. A*, 2007, **127**, 21430.

13 H. D. Burrows, *Inorg. Chem*, 1990, **3**, 139; H. D. Burrows and T. Kemp, *Chem. Soc. Rev.*, 1974, **3**, 139; C. Görller-Walrand and K. Servaes, *Helv. Chim. Acta*, 2009, **92**, 2304; R. Ghosh, J. A. Mondal, H. N. Gosh and D. K. Palit, *J. Phys. Chem. A*, 2010, **114**, 5263; R. Nagaishi, Y. Katsumura, K. Ishigure, H. Aoyagi, Z. Yoshida, T. Kimura and Y. Kato, *J. Photochem. Photobiol., A*, 2002, **146**, 157; S. J. Formosinho, H. D. Burrows, M. G. M. Miguel, M. E. D. G. Azenha, I. M. Saraiva, A. Catarina, D. N. Ribeiro, I. V. Kholyakov, R. G. Gasanov, M. Bolte and M. Sarakhad, *Photochem. Photobiol. Sci.*, 2003, **2**, 569.

14 Tsushima, *Inorg. Chem.*, 2009, **48**, 4856; S. Tsushima, C. Götz and K. Fahmy, *Chem Eur J*, 2010, **16**, 8029.

15 H. D. Burrows and M. G. M. Miguel, *Adv. Colloid Interface Sci.*, 2001, **89–90**, 485; M. Lopez and D. J. S. Birch, *Analyst*, 1996, **121**, 905; V. Sladkov, B. Fourest and F. Mercier, *Dalton Trans.*, 2009, 7734; A. Günther, G. Geipel and G. Bernhard, *Polyhedron*, 2007, **26**, 59; S. Maji and K. S. Viswanathan, *J. Lumin.*, 2009, **129**, 1242; I. Billiard, *et al.*, *Appl. Spectrosc.*, 2003, **57**, 1027; N. W. Hayes, C. J. Tremblett, P. J. Melfi, J. D. Sessler and A. M. Shaw, *Analyst*, 2008, **133**, 616; J. Liu, A. K. Brown, X. Meng, D. M. Cropek, J. D. Istok, D. B. Watson and Yi Lu, *Proc. Natl. Acad. Sci. U. S. A.*, 2007, **104**, 2056; D. Pestov, C.-C. Chen, J. D. Nelson, J. E. Anderson and G. Tepper, *Sens. Actuators, B*, 2009, **138**, 134.

16 See for example:G.-L. Law, D. Parker, S. L. Richardson and K.-L. Wong, *Dalton Trans.*, 2009, 8481; A. P. de Silva, H. Q. N. Gunaratne, T. E. Rice and S. Stewart, *Chem. Commun.*, 1997, 1891; S. Mizukami, K. Tonai, M. Kaneko and K. Kikuchi, *J. Am. Chem. Soc.*, 2008, **130**, 14376; G. Muller, *Dalton Trans.*, 2009, 9692; D. Parker, P. K. Senanayake and J. A. G. Williams, *J. Chem. Soc., Perkin Trans. 2*, 1998, 2129; M. P. Lowe, D. Parker, O. Reany, S. Aime, M. Botta, C. Castellano, E. Gianolio and R. Pagliarin, *J. Am. Chem. Soc.*, 2001, **123**, 7601; S. J. A. Pope and R. H. Laye, *Dalton Trans.*, 2006, 3108.

17 Examples of emissive uranyl complexes under ambient conditions include: Z. Hnatejko, S. Lis and Z. Stryła, *J. Therm. Anal. Calorim.*, 2009, **100**, 253; R. Steudtner, T. Arnold, G. Geipel and G. Bernhard, *J. Radioanal. Nucl. Chem.*, 2010, **284**, 421.

18 F. de Maria Ramirez, S. Varbanov, J. Padilla and J.-C. G. Bünzli, *J. Phys. Chem. B*, 2008, **112**, 10976.

19 T. Yayamura, S. Iwata, S. I. Iwamaru and H. Tomiyasu, *J. Chem. Soc., Faraday Trans.*, 1994, **90**, 3253; S. Kannan, M. A. Moody, C. L. Barnes and P. B. Duval, *Inorg. Chem.*, 2006, **45**, 9206; A. E. Vaughn, D. B. Bassil, C. L. Barnes, S. A. Tucker and P. B. Duval, *J. Am. Chem. Soc.*, 2006, **128**, 10656.

20 G. R. Choppin, J-O. Liljenzin, J. Rydberg, *Radiochemistry and Nuclear Chemistry*, 3rd edition, 2002, Butterworth-Heinemann, USAA. P. Paiva, P. Malik, *J. Radioanal. Nucl. Chem.*, 2004, 261, 485.

21 A. Cousson, S. Debos, H. A. Dazli, F. Nectoux, M. Pogu and G. R. Choppin, *J. Less Common Met.*, 1984, **99**, 233; C. Madic, B. Guillame, J. C. Morriseau and J. P. Moulin, *J. Inorg. Nucl. Chem.*, 1979, **41**, 1027; J. L. Sessler, A. E. V. Gorden, R. J. Donohoe, C. Drew Tait and D. Webster Keogh, *Inorg. Chim. Acta*, 2002, **341**, 54; A. E. V. Gorden, J. Xu, K. N. Raymond and P. Durbin, *Chem. Rev.*, 2003, **103**, 4207; A. A. Bessonov, N. N. Krot, M. S. Grigor'ev and V. I. Makarenkov, *Radiochemistry*, 2005, **47**, 468; S. D. Reilly and M. P. Neu, *Inorg. Chem.*, 2006, **45**, 1839; S. M. Cornet, L. J. L. Hadler, M. J. Sarsfield, D. Collison, M. Helliwell, I. May and N. Kaltsoyannis, *Chem. Commun.*, 2009, 917; S. Skanthakumar, M. R. Antonio and L. Soderholm, *Inorg. Chem.*, 2008, **47**, 4591.

22 M. Latva, H. Takalo, V.-M. Mukkala, C. Matachescu, J. C. Rodriguez-Ubis and J. Kankare, *J. Lumin.*, 1997, **75**, 149; D. Parker, P. K. Senanayake and J. A. G. Williams, *J. Chem. Soc., Perkin Trans. 2*, 1998, 2129.

23 M. J. Sarsfield, I. May, S. M. Cornet and M. Helliwell, *Inorg. Chem.*, 2005, **44**, 7310.

24 M. P. Wilkerson, C. J. Burns, R. T. Paine and B. L. Scott, *Inorg. Chem.*, 1999, **38**, 4156.

25 G. Bombieri, E. Forsellini and J. P. Day, *J. Chem. Soc., Dalton Trans.*, 1978, 677.

26 J. L. Häller, N. Kaltsoyannis, M. J. Sarsfield, I. May, S. M. Cornet, M. P. Redmond and M. Helliwell, *Inorg. Chem.*, 2007, **46**, 4868.

27 F. A. Arnáiz, M. J. Miranda, R. Aguada, J. Mahía and M. A. Maestro, *Polyhedron*, 2001, **20**, 3295.

28 The apparent electronic origin values ($E_{0\text{-}0}$) were determined from the observed energy of the first vibronic band in the emission spectra. The exact location of $E_{0\text{-}0}$ however, is often difficult to ascertain in spectra of $\{UO_2^{2+}\}$ compounds especially at low resolution. The exact $E_{0\text{-}0}$ may lie at higher energies depending on the local symmetry of the complex in question.

29 Z. Fazekas, T. Yamamura and H. Tomiyasu, *J. Alloys Compd.*, 1998, **271–273**, 756.

30 M. E. D. G. Azenha, H. D. Burrows, S. J. Formosinho, M. G. M. Miguel, A. P. Daramanyan and I. V. Kholyakov, *J. Lumin.*, 1991, **48–49**, 522.

31 R. Bradshaw, D. Sykes, L. S. Natrajan, R. J. Taylor, F. R. Livens and S. Faulkner, IOP Conference Series, *Materials Science and Engineering*, 2010, **9**, 012047.

32 R. Cea-Olivares, G. Canseco-Melchor, M. M. Moya-Cabrera, V. Garcia-Montalvo, J. G. Alvarado-Rodriguez and R. A. Toscano, *Inorg. Chem. Commun.*, 2005, **8**, 205.

33 M. J. Sarsfield, M. Helliwell and J. Raftery, *Inorg. Chem.*, 2004, **43**, 3170.

34 P. L. Arnold, D. Patel, C. Wilson and J. B. Love, *Nature*, 2008, **451**, 315; P. L. Arnold, A.-F. Pécharman, E. Hollis, A. Yahia, L. Maron, S. Parsons and J. B. Love, *Nat. Chem.*, 2010, **2**, 1056.

35 M. P. Wilkerson, C. J. Burns, H. J. Dewey, J. M. Martin, D. E. Morris, R. T. Paine and B. L. Scott, *Inorg. Chem.*, 2000, **39**, 5277.

36 A. P. Bassett, R. Van Deun, P. Nockemann, B. Glover, B. M. Kariuki, K. Van Hecke, L. Van Meervelt and Z. Pikramenou, *Inorg. Chem.*, 2005, **44**, 6140; S. W. Magennis, S. Parsons and Z. Pikramenou, *Chem.–Eur. J.*, 2002, **8**, 5761; S. W. Magennis, S. Parsons, A. Corval, J. D. Woollins and Z. Pikramenou, *Chem. Commun.*, 1999, 61; P. B. Glover, A P. Bassett, P. Nockemann, B. M. Kariuki, R. Van Deun and Z. Pikramenou, *Chem.–Eur. J.*, 2007, **13**, 6308.

37 A. Carvalho, V. G.-Montalvo, A. Domingos, R. Cea,.-Olivares, N. Marques and A. Pires, de Matos, *Polyhedron*, 2000, **19**, 1699.

38 K. Bokolo, A. Courtois, J.-J. Delpuech, E. Elkaim, D. Rinaldi, L. Rodehüser and P. Rubini, *J. Am. Chem. Soc.*, 1984, **106**, 6333.
39 L. H. Jones, *Spectrochim. Acta*, 1958, **10**, 395; C. N. Trung, G. M. Begun and D. A. Palmer, *Inorg. Chem.*, 1992, **31**, 5280.
40 D. L. Clark, S. D. Conadson, R. J. Donohoe, D. W. Keogh, D. E. Morris, P. D. Palmer, R. D. Rogers and C. D. Tait, *Inorg. Chem.*, 1999, **38**, 1456.
41 G. Meinrath, *J. Radioanal. Nucl. Chem.*, 1997, **224**, 119.
42 C. Moulin, I. Laszak, V. Moulin and C. Tondre, *Appl. Spectrosc.*, 1998, **52**, 528; D. E. Morris, C. J. Chisholm-Brause, M. E. Barr, S. D. Conradson and P. G. Eller, *Geochim. Cosmochim. Acta*, 1994, **58**, 3613.
43 R. O. Day, R. R. Holmes, A. Schmidpeter, K. Stoll and L. Howe, *Chem. Ber.*, 1991, **124**, 2443.
44 G. M. Sheldrick, *SHELXTL 5.04*, An integrated system for solving, refining and displaying crystal structures from diffraction data, Siemens Analytical X-ray Instruments Inc., Madison, WI, 1995PLATON; A. L. Speck, *Acta Crystallogr. Sect. A*, 1990, **46**, C34; G. M. Sheldrick, *Acta Crystallogr., Sect. A: Found. Crystallogr.*, 2007, **A64**, 112.
45 I. M. Clarkson, A. Beeby, J. I. Bruce, J. L. Govenlock, M. P. Lowe, C. E. Mathieu, D. Parker and K. Senanayake, *New J. Chem.*, 2000, **24**, 377; R. A. Poole, G. Bobba, M. J. Cann, J.-C. Frias, D. Parker and R. Peacock, *Org. Biomol. Chem.*, 2005, **3**, 1013.

